On the origin of high-temperature superconductivity in cuprates

I. Božović*[a,b], J. Wu[a], X. He[a,b] and A. T. Bollinger[a]

[a]Brookhaven National Laboratory, Upton, New York 11973-5000, USA
[b]Yale University, Applied Physics Department, New Haven CT 06520, USA

ABSTRACT

Here we review the results of a comprehensive study of high-temperature superconductivity in cuprates that took over ten years to complete. It required development of the technique, for synthesis as well as for measurements of the key physical properties of the superconducting and the normal states, in order to establish their precise dependence on doping, temperature, and external fields. We use atomic-layer-by-layer molecular beam epitaxy to synthesize atomically perfect thin films and multilayers of high-T_c cuprates. We use the mutual inductance technique refined to measure the absolute value of penetration depth λ to accuracy better than 1%. We have synthesized and studied over 2,000 cuprate films. The large statistics reveals clear trends and intrinsic properties; this is essential when dealing with complex materials such as cuprates. The findings bring in some great surprises, challenge the commonly held beliefs, rule out many models, and point to an unexpected answer to the question why is T_c so high in cuprates.

Keywords:

1. INTRODUCTION

Intense study of high-temperature superconductivity (HTS) in cuprates has brought about numerous intriguing questions — about the nature and the role of the 'anomalous normal state', of the pseudogap, of competing instabilities such as spin and charge density waves, etc.[1-3] Nevertheless, we maintain that the foremost mystery is just why the critical temperature (T_c) is so high, reaching 165 K under high pressure[4]. The fundamental dichotomy is between the weak-pairing, Bardeen-Cooper-Schrieffer (BCS) scenario, and Bose-Einstein condensation (BEC) of strongly-bound pairs. While for underdoped cuprates it is hotly debated which of these pictures is appropriate, it is commonly believed that on the overdoped side strongly-correlated fermion physics evolves smoothly into the conventional BCS behavior.

We have tried to probe this question by the following strategy, focused on the overdoped side of the cuprate phase diagram. In this region, large Fermi surfaces have been depicted by angle-resolved photoemission spectroscopy (ARPES)[5] as well as by the Fourier-transformed scanning tunneling microscopy (STM)[6]. Moreover, the thermal and electrical conductivity were found to follow the standard Wiedemann-Franz law[7]. Hence, today it is almost universally believed that in cuprates the physics of strongly correlated fermions evolves smoothly upon overdoping into the conventional situation in which the normal state is well described by Landau's Fermi Liquid theory and the superconducting state by the BCS theory.

If this is the case, then we have a well-understood fixed point from which to start our probing, and could try following the evolution of the system, as continuously as possible, as the doping is reduced towards the composition with the maximal T_c. One can envision two possible outcomes of such an experiment. We may find that all the relevant observables that characterize the normal and the superconducting states evolve smoothly and monotonously all the way up to the optimal doping. In this case, one would infer that even in the material with the maximal T_c the ground state wave function ought to be BCS-like in its broad (topological) features, albeit perhaps 'distorted' by strong coupling. Indeed, this view has been advocated by many authors, and most prominently in a recent tour-de-force work of R. Laughlin[8,9]. Alternatively, we may encounter some jumps, discontinuities and singularities on our way towards the top of the T_c dome, in which case the ground state there could be of a qualitatively different nature.[10]

With this motivation, we have embarked upon the task of synthesizing and studying a large set of cuprate samples, varying the doping level as continuously as possible, and testing whether the key superconducting parameters scale with doping and temperature as expected from the BCS theory. As we anticipated, we have found that the evolution is quite smooth, without any apparent jumps. However, surprisingly, the findings do not conform to the BCS predictions anywhere in the phase diagram.

*bozovic@bnl.gov; phone 1 (631) 344-4973; fax 1 (631) 344-4071; www.bnl.gov/cmpmsd/mbe

In contrast to the normal state, the superconducting state in cuprates appears to be comparatively simple and featureless. It can be described by a few essential parameters, such as T_c and the magnetic penetration depth λ the characteristic length scales over which the magnetic field and the order parameter, respectively, can vary. By measuring the temperature and doping dependences of λ and checking its relation to T_c, we can test whether the BCS predictions are fulfilled.

Important tests include (a) the temperature dependence of the superfluid electron density $n_s = m^*/\mu_0 e^2 \lambda^2$, where $\mu_0 = 4\pi \times 10^{-7} N/A^2$ is the vacuum permeability, e the electron charge, and m^* the effective electron mass, (b) the doping dependence of $n_{s0} = n_s(T \to 0)$, and (c) the dependence of Tc on n_{s0}. In BCS theory, one would expect (a) $n_s(T)$ to dive downwards when $T \to T_c$ as the gap closes, i.e., it should be convex; (c) n_{s0} should be essentially equal to the mobile charge carrier density in the normal state and hence in highly overdoped cuprates it should reach ~ 0.7 holes per Cu, as indicated by the theory[9] and by the Fermi surface area determined experimentally[5,6], and (c) there is no direct relation between n_{s0} and T_c. (Some of these statements would need to be modified for dirty BCS superconductors, but in what follows we demonstrate that our LSCO films show behavior consistent with London (local) electrodynamics in the clean limit.) In contrast, if superconductivity was due to BEC, pairs could exist (and stay small) well above T_c. In this case, (a) $n_s(T)$ may be concave or stay linear or all the way to T_c; (b) $n_{s0}/2$ should be equal to the density of preformed pairs, and (c) Tc should increase with n_{s0} monotonously.[11-13]

2. EXPERIMENTAL

Our technical goal was to measure λ with a high absolute accuracy in a large set of LSCO films, varying the doping level in small increments. This task posed many technical challenges, which we were able to meet eventually. Our, technique for film synthesis is based on atomic-layer-by-layer molecular beam epitaxy (ALL-MBE).[14-17] For this study, we have chosen $La_{2-x}Sr_xCuO_4$ (LSCO), since it is the simplest among the HTS cuprates, and because we can dope it all the way to non-superconducting metal. Our focus here is on the overdoped LSCO, which is believed to be simpler, since on the underdoped side there are many competing or intertwined phases. Since we have shown earlier that HTS can occur in a single CuO_2 plane[16] with T_c equal to what is seen in bulk samples, we take it that the essential physics is quasi-two-dimensional (2D), and hence we restrict our study to in-plane properties here.

The main uncertainties in many (if not most) HTS experiments so far have been sample-related. Most cuprate samples are inhomogeneous at some level. For example, most HTS single crystals contain stacking faults and inclusions of other cuprate phases. Since oxygen is volatile in most cuprates, gradients in the density of oxygen vacancies or interstitials are essentially ubiquitous. Additional uncertainty in measurements of transport properties of bulk crystals may come from irregular geometry or from the contacts. These problems can be avoided by studying very thin films. Regrettably, HTS films synthesized by most techniques tend to be granular and riddled with pinholes and secondary-phase inclusions. This motivated our efforts to improve the synthesis technique as well as to study large sample sets, providing for enough statistics to identify clear trends and discern intrinsic properties and phenomena.

Our main tool for this film synthesis is a custom atomic-layer-by-layer molecular beam epitaxy (ALL-MBE) system equipped with 16 thermal effusion cells as metal sources, a pure ozone source, a reflection high-energy electron diffraction (RHEED) system, and other in-situ analytical tools.[14] Real-time information about the film surface morphology, chemical composition, and crystal structure allows synthesis of single-crystal this films, with atomically smooth surfaces and interfaces. Using this system, we have performed over 2,500 LSCO film growth experiments so far. We characterize every film in real time by RHEED, which provides a digital count of atomic layers from RHEED oscillations. Every film was characterized ex situ by Atomic Force Microscopy (AFM) and magnetic susceptibility measurements, and selected films also by TOF-ISARS, X-ray diffraction (XRD), transport measurements, etc. In close collaboration with other groups at BNL and elsewhere, many of our films were also characterized by transmission electron microscopy, electron energy loss spectroscopy, resonant elastic and inelastic synchrotron X-ray scattering, ultrafast electron diffraction, ultrafast optical and THz pump-probe techniques, muon spin resonance, etc.

Addressing the problem of oxygen non-uniformity, we have performed more than a thousand annealing experiments, in ozone, oxygen, or vacuum, spanning 13 orders of magnitude in oxygen partial pressure. Each of these films were characterized by AFM, transport, and XRD, both before and after each annealing step, the. These comprehensive studies generated our 'recipes', consisting of specific annealing cycles at different temperature and pressure, to produce films with the sharpest superconducting transitions, and the most homogeneous as judged by other physical properties.

Another major problem that limits the accuracy of mutual inductance measurements is uncertainty in the thickness of the superconducting layer. ALL-MBE provides digital control over the film thickness, but the actual thickness of the superfluid may be smaller, because a couple of layers next to the substrate and near the free film surface (if the film has been exposed to atmosphere) are modified structurally and chemically and are not superconducting. We solve this this problem by atomic-layer engineering, as illustrated in Figure 1. An exactly 5 unit cells (5 UC) thick HTS layer is superconducting. We protect it from below by a metallic ($M = La_{1.60}Sr_{0.40}CuO_4$) buffer and from above by a cover layer. Still, some hole depletion from M and accumulation in the nearest HTS layers[15] can occur. To minimize this interfacial effect, we grade Sr doping in the layers near the interface to engineer the charge profile. Finally, to quench any potential residual superconductivity and eliminate any interface contributions, we dope these transition layers by substituting 3% of Cu with Zn. (Zn doping suppresses[16] T_c by a factor of two and N_s by a factor of four.) To test the validity of this approach, we studied a series of films in which the central HTS layers thickness was varied over a broad range, while keeping the same composition of the constituent materials. We found that the sheet superfluid density scaled linearly with the thickness of the HTS layer, as indeed expected.
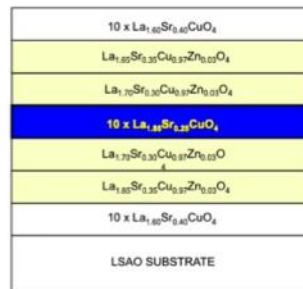

Figure 1. A schematic of sample engineered for this study at the atomic-layer level. The active (superconducting) part of the film consists of a 5 unit cells (UC) thick layer of $La_{2-x}Sr_xCuO_4$. It is protected by a 6 UC thick, metallic but non-superconducting $La_{1.60}Sr_{0.40}CuO_4$ buffer to isolate it from the substrate, and by another 6 UC thick $La_{1.60}Sr_{0.40}CuO_4$ overlayer to protect it from the atmosphere. In the two layers next to the interfaces, the Sr doping level is graded and 3% of Cu is substituted by Zn to quench interface superconductivity.

Turning now to measurements of λ, the most common techniques include muon spin resonance (μSR), microwave resonance (cavity-perturbation), or inductance techniques. Usually, μSR measurements are performed at just a few compositions and temperatures, given the duration and cost of these experiments. On the other hand, uncertainty in geometric factors limits the absolute accuracy of the microwave technique. Hence, we have chosen the mutual inductance method[18-23], pioneered by A. Hebard and A. Fiory[18], J. Claasen[19], and T. Lemberger[21,22] (Figures 2a and 2b). This technique is best suited for thin film studies, but we found that numerous technical improvements were necessary to eliminate the main sources of error, and reach our desired absolute accuracy.

In every mutual inductance scheme, that is some parasitic field coupling around the film and through the electronics. To minimize field leakage around the film, we use micro-machined inductance coils with a large number of turns (300-1,500) but very small inner radius (250 μm), much smaller than the film size (10×10 mm^2), so this parasitic signal is very small (< 0.3%). Nevertheless, we measure this leakage accurately using thick films of Nb, Pb, and Al, through which transmittance is negligible, deposited on the same substrates, and then we subtract this from the measured signal. As yet another check, we cover the HTS film with a thick layer of Al, cool it down to T = 0.3 K, and then turn the diamagnetic screening in Al on and off by switching a small (100 Gauss) dc magnetic field; this does not affect the HTS film but is sufficient to drive Al normal. Next, we checked that the (corrected) N_{s0} is independent on frequency and scales linearly with the film thickness. (The leakage contribution varies with linearly with frequency and can be separated that way.) The sample holder is carved out of a single block of sapphire crystal, in order to minimize eddy currents. Inside the sapphire holder, the coils are fixed rigidly by epoxy, so that they do not move. The sample is spring-loaded in such a way that the film surface is always positioned in exactly the same way. The overall system reproducibility is ±0.3%, even for measurements repeated a year later.

After these corrections, due to some small difference in the actual coil geometry and its mathematical ideal, our measured mutual inductance $M(T)$ may differ by a couple per cent from the calculated one. To compensate for this multiplicative factor, we normalize the measured $M(T)$ by its value M_{high} just above T_c. Next, to double-check for the possibility of field penetration through secondary-phase grains and/or pinholes, we synthesized and studied ultrathin films, down to 1 UC thick. Next, in the literature it has been common to measure λ down to T = 4 K only and extrapolate the data to T→0. This may bring in some error, especially for films with very low T_c, which however are most relevant to unravel the behavior near the quantum critical point where T_c vanishes. With this in mind, we have built a He-3 based setup that allows us to measure λ down to 300 mK. To ensure accurate temperature reading, we use a very low (0.2 K/min) ramp rate, while the thermal stability in our setup is better than 1 mK; in addition, we measure $\lambda(T)$ upon both cooling and heating. Altogether, the absolute accuracy of our λ measurements is better than 1%, while the relative values of $\lambda(T)$, on which much of our conclusions are based, are accurate to better than 0.1%.

We also checked and verified a good agreement between our low-frequency (1 – 100 kHz) results shown here and the high-frequency (0.5 – 50 MHz) inductance measurements in the reflectance geometry[23] in our laboratory, and the THz and μSR data measured on our films by collaborating groups.

So far, we have performed inductance measurements on more than 2,500 LSCO films, a number of which were measured dozens of times and on multiple (the total of ten so far) setups. Mining this large database allows one to identify clear statistical trends and uncover intrinsic behavior. Here, we focus on the films with the sharpest transitions; in the best ones, near T_c we see $\text{Re}\sigma(\omega, T)$ rising exponentially on the scale of 0.1-0.2 K. This puts an upper bound on any inhomogeneity in T_c, since the transition width comes largely from thermal fluctuations. Clearly, these samples are very homogeneous, and hence they can be presumed to display intrinsic properties and behavior.

From the measured λ, we calculate the superfluid stiffness $\rho_s = d/\lambda^2$, where $d = 0.662$ nm, so ρ_s is also determined directly and free of any assumptions. Just to facilitate communication, we also introduce the (dimensionless) superfluid density, i.e., the number of superconducting carriers per formula unit, given by $N_s = (m^* a_0^2/\mu_0 e^2)\rho_s$ where $a_0 = 0.38$ nm and $\mu_0 = 4\pi \times 10^{-7}$ H/m, and assuming the pair mass $m_p = 2m^* = 4m_e = 3.6 \times 10^{-30}$ kg. Note, however, that none of our conclusions are dependent on this assumption. ARPES and optics studies indeed showed that in LSCO m^* is essentially constant across the entire phase diagram. Our own $\rho(T, x)$ data show that as the doping is increased the resistivity decreases monotonously and smoothly; this rules out any significant increase in m^* when p increases, and in particular, a divergence in m^* when $p \to p_{c2}$.
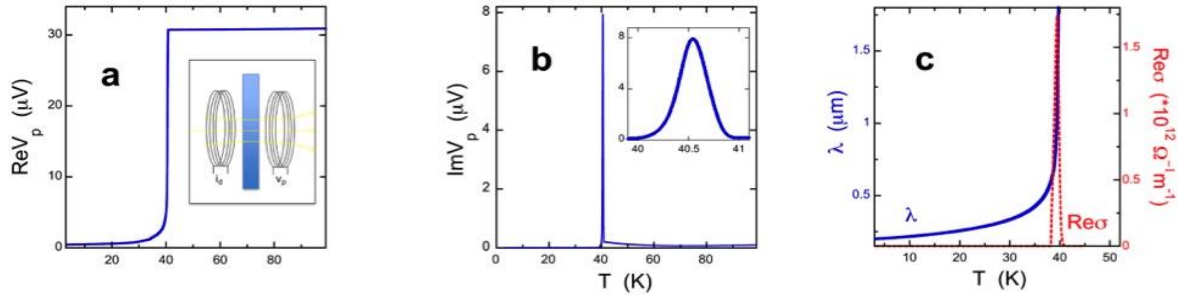

Figure 2. **a**, The real part of emf in the pickup coil (proportional to the mutual inductance) showing diamagnetic screening (the Meissner effect) when the film becomes superconducting. The schematic of the experiment is shown in the inset. **b**, The imaginary part of V_p shows that in this film, of 10×10 mm^2 area, T_c is homogeneous to better than 0.1 K. **c**, The penetration depth λ and the ac ($\nu = 40$ KHz) conductivity derived from the complex impedance

In Figures 2a-2c, we show as an example the raw data from a mutual inductance measurement on an optimally doped LSCO film synthesized by ALL-MBE. The sharpness of the peak in $\text{Im}V_p(T)$, or equivalently in $\text{Im}M(T)$, is a measure of the sample homogeneity. In this film, as T_c is approached from above, the ac conductivity grows exponentially with the characteristic temperature scale of ~0.1 K. This is an upper bound on the spread in T_c in this film (of 10×10 mm^2 area). Here, we define T_c as the temperature at which the $\text{Re}M(T)$ starts to drop and $\text{Im}M(T)$ starts to rise — the onset of the Meissner effect. It coincides with the temperature at which the film resistance drops to zero (i.e., to the noise floor in dc resistance measurements). The broadening of the resistive transition is intrinsic and comes from flux flow that occurs in the region above T_c and below some T_c^{onset}, which is typically about 10 K higher.

In a similar manner, we have studied a very large sample set. We have measured inductance in over 2,000 LSCO films, varying the composition across the entire phase diagram and the thickness from 0.66 nm (one-half unit cell) to over 100 nm. This was decisive – cuprates are complex compounds, and HTS has largely been a materials-science endeavor. Our large statistics allows us to identify clear trends and discern intrinsic behavior.

2.1 Experimental results: An example of a heavily overdoped LSCO film

To get the message across, let us first consider one example — a film with $p = 0.25$ and $T_c = 6$ K, heavily overdoped to very near the quantum critical point at $p_{c2} = 0.26$. (NB: the values of p quoted here, and in the literature, are only approximately equal to the mobile carrier (hole) density. However, this affects none of our conclusions, all of which exclusively rest on the quantities such as T_c, λ, etc., that we measure directly and accurately.) According to the accepted wisdom, this sample should be deep inside the region where the superconducting state is well described by the BCS theory, while the normal state should behave as a *bona fide* Fermi Liquid. The resistance of this film indeed shows the canonic $\rho(T) \propto T^2$ dependence starting just above T_c.
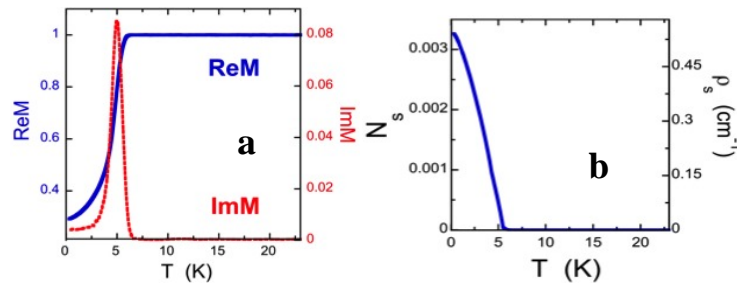

Figure 3. **a**, The real and the imaginary part of mutual inductance (normalized to the normal-state value) in a heavily overdoped ($p = 0.25$) LSCO film. **b**, Right scale: the superfluid stiffness $\rho_s = d/\lambda^2$, where $d = 0.662$ nm. Left scale: the number of superconducting carriers per formula unit, N_s. Note that here N_s^0 is two orders of magnitude smaller than expected from the BCS theory.

In Figure 3a we display the inductance measurement data, showing that the superconducting transition is quite sharp. The dependence of the superfluid density (normalized to one LSCO formula unit) on temperature is shown in Figure 3b; it is smooth and shows no kinks.

2.2 Experimental results: The data for the entire sample set and the phase diagram

Having clarified our methodology, we now show the results for the whole battery of samples, covering densely the entire overdoped LSCO region with the hole concentration varied from $p = 0.16$ all the way to $p_{c2} = 0.26$ and beyond. In Figure 4, we display the doping dependence of $\lambda(T)$ for the one hundred best, most homogeneous LSCO films, with the sharpest transitions (HWHM of Im$M(T)$ peak less than 0.5 K). Figures 5a and 5b show the doping dependence of $N_s(T)$. The later gives the dependence of N_{s0} on doping as depicted in Figure 6; for comparison, we also show the predictions based on BCS theory[9]. The discrepancy is vast and appears irreconcilable. Figure 7 shows the dependence of T_c on N_{s0}.
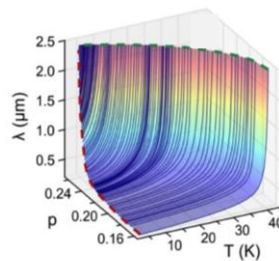

Figure 4. The $\lambda(T)$ data for the one hundred most homogeneous LSCO films grown by ALL-MBE.

Our main observations are as follows.

(i) When $p \rightarrow p_{c2}$, both $T_c \rightarrow 0$ and $N_{s0} \rightarrow 0$. (Fig. 5)

(ii) The $N_s(T)$ curves are for the most part linear, $N_s(T) = N_{s0} - AT$ with $A = const.$ (Fig. 5)

(iii) Variations in T_c within a single LSCO film are very small ($<< 1$ K); every film is quite homogeneous. (Figs. 2, 3a)

(iv) The $T_c(N_{s0})$ dependence is linear but with a clear offset, $T_c = T_0 + \alpha N_{s0}$, where $T_0 = (7 \pm 0.1)$K and $\alpha = (2.5 \pm 0.1) \times 10^2$K, except very close to the origin (i.e., for $N_{s0} < 0.02$) where it fits to $T_c = \gamma \sqrt{N_{s0}}$, with $\gamma = (1.1 \pm 0.1) \times 10^2$K (Fig. 7)
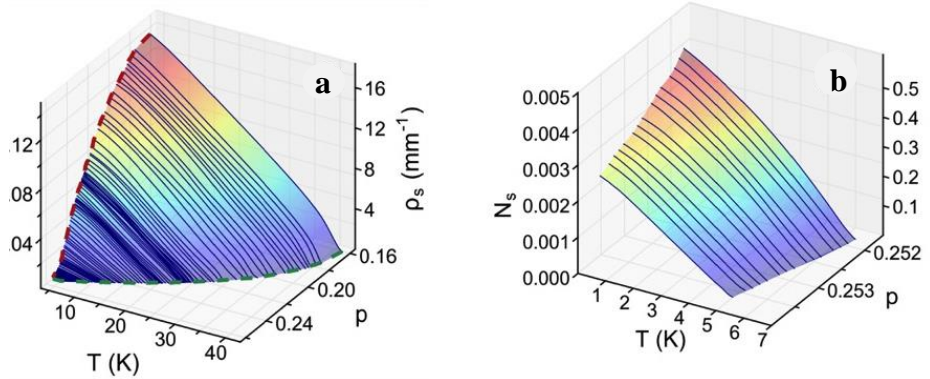

Figure 5. a, The corresponding $N_s(T)$ curves (left scale) or $\rho_s(T)$ curves (right scale) are for the most part essentially linear. In some samples, small deviations from linearity are seen at very low T and/or also very (1-2 K) close to T_c. **b**, The same, but zoomed in on the most overdoped samples, measured down to $T = 0.3$ K.

3. DISCUSSION

Our findings (i)-(iv) are very specific, and at variance with numerous proposed models for HTS in cuprates. First, they are at odds with the BCS theory in any variant, clean or dirty, including the Migdal-Eliashberg theory, generalizations that postulate pairing by exchange of virtual magnons, excitons, plasmons, etc. Next, they are at variance with ascribing the dependence of Ns on temperature and doping across the entire phase diagram to quantum phase fluctuations associated with the quantum critical points (QCP) at the dome edges ($p_{c1} = 0.06$ and $p_{c2} = 0.26$) or with a 'hidden' QCP at $p \approx 0.19$. As for thermal phase fluctuations, we see no evidence of the Berezinskii-Kosterlitz-Thouless (BKT) transition, even when the superfluid is confined to a single CuO_2 plane[16], except at very high (MHz) frequencies[23]. Our data also show deviations from the scaling laws proposed on phenomenological grounds[30,31]. We see no evidence of a d-wave to s-wave crossover, $d+is$, $d+id$, two-band behavior, etc., all of which have been proposed.
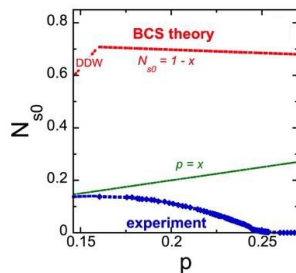

Figure 6. The dependence of N_{s0} on doping, compared to the dependence expected[9] within a BCS picture (which also incorporates the d-density wave, DDW, a postulated competing instability), across the entire overdoped region. The disagreement seems irreconcilable.

Finally, we can also rule out the presence of a large density of pair-breaking impurities or structural defects, of electronic or chemical phase separation, and of a broad distribution of gap values (such as seen in $Bi_2Sr_2CaCu_2O_8$ by STM); the superconducting fluid in our LSCO films appears to be quite homogeneous. The key arguments are that (a) Tc is sharp and uniform down to 0.1 K in the best films, (b) $N_s(T)$ stays linear down to very low T — to 1-2 K in the best samples, and (c) the mean free path near T_c is much larger than the coherence length ξ. The evolution of the superconducting state with doping, from optimal all the way to overdoped non-superconducting metal, appears monotonous and smooth. The same is in fact true of the normal state, as judged by our equally extensive data set on the key transport properties such as ρ, ρ_H, and magnetoresistance, but a detailed account requires much space and has to be reported separately.
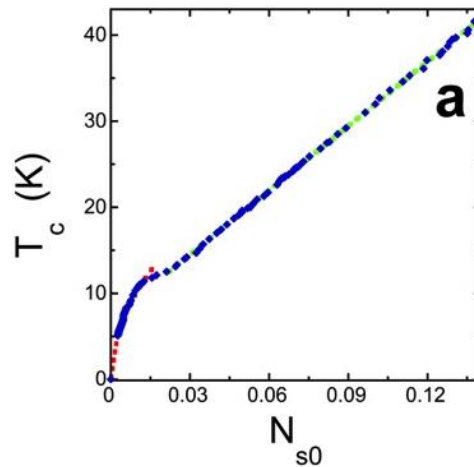

Figure 7. The relation between T_c and $N_0 \equiv N_s(T \rightarrow 0)$ (experimental data: solid blue diamonds). For $N_{s0} > 0.03$, the dependence is linear but with a clear offset, $T_c = T_0 + \alpha N_{s0}$, where $T_0 = (7 \pm 0.1)$ K, and $\alpha = (2.5 \pm 0.1) \times 10^2$ K, (fit: green dashed line). In the narrow region near the origin (for $N_{s0} < 0.02$), the curve fits well to $T_c = \gamma \sqrt{N_{s0}}$, with $\gamma = (1.1 \pm 0.1) \times 10^2$ K (fit: red dashed line).

Tellingly, the present data strongly indicate that the pairs are small (local), as if we were on the BEC side of the crossover. Assuredly, BCS and BEC models have much in common zero resistance, Meissner effect, flux quantization, vortices, Josephson effects - since all that follows just from the broken gauge symmetry[32]. Indeed, theory indicates that BCS should crossover smoothly to BEC as the pairing interaction is increased[27-29,33-36]. Experimentally, both BEC and BCS have been observed in ultra-cold trapped gases of fermionic atoms, as the pairing interaction strength is tuned[37-42]. When the pairing is weak, the typical BCS behavior is seen; as the interaction is boosted up the pair size shrinks until local pairs (i.e., diatomic molecules) are formed, and a crossover to BEC occurs[39-41]. Nevertheless, there are also profound differences between BCS and BEC that actually matter here.

In a Fermi liquid, Pauli exclusion keeps most electrons frozen inside the Fermi sphere, while only a small fraction (in the narrow Debye shell, about k_BT/E_F wide) is perturbed by thermal agitation. In BCS superconductors, condensation is driven by a reduction in the potential energy, and it is exponentially small, so consequently the same is true of T_c. In contrast, in BEC a large fraction of bosons — essentially all for $T \rightarrow 0$ and a weak interaction — can occupy the same state, so they all contribute to condensation, which is largely driven by a reduction in the kinetic energy; everything else being the same, this results in a much higher T_c. Thus, in He-4, which is bosonic, superfluidity persists up to $T_c = 2.17$ K, two orders of magnitude higher than in He-3 ($T_c \approx 30$ mK), which is fermionic[12].

Dimensionality also differentiates between BCS and BEC. In a three-dimensional (3D) potential well, bound states do not form unless the well is deep enough, while in 2D they form in arbitrarily shallow wells; thus, 3D favors BCS while 2D favors BEC. Indeed, a dimensional crossover from BCS to BEC can be triggered just by making the cold-atom cloud thinner[42]. Notably, in a 2D Bose gas N_s is indeed predicted[43,44] to decrease linearly with T.

Thus, (a) the strong pairing, (b) the high T_c, and (c) the 2D nature of superconductivity in cuprates a priori all point to BEC rather than to BCS. Accordingly, BEC has been invoked in numerous theories of HTS in cuprates.[10,45-50] Our data presented here provide some support to this general viewpoint. However, a large body of other experimental data, notably including ARPES, STM, quantum oscillations, etc., indicates the presence of fermions, the density of which increases with doping, concomitantly with the decrease in Tc. Indeed, we see that the normal-state conductivity increases with doping, even while N_{s0} decreases to zero. The big surprise is that all these fermions apparently do not participate in the superfluid, even at $T = 300$ mK. The challenge to theory is to integrate these apparently conflicting aspects, which may require a new model. The ultimate microscopic theory should also explain how pairs form at such high temperatures, what makes cuprates so exceptional in this respect, what is the relation between the pseudogap and pairing, and why is the $N_{s0}(p)$ dependence dome-shaped.

4. CONCLUSION AND OUTLOOK

We have determined the dependence of the key superconducting parameters, $\lambda(T,p)$, and $\xi(T,p)$, on temperature and doping, and extracted the $T_c(N_{s0})$ dependence, covering densely the entire optimally-doped to overdoped side of the LSCO phase diagram. The observed dependences disagree with the BCS predictions qualitatively and quantitatively, the discrepancy reaching a few orders of magnitude. Rather, the data indicate that strong interactions lead to formation of pairs that are small (local) and 'preformed', i.e., present well above T_c where they undergo BEC. These bosons are charged and very light, with the mass on the order of an electron mass, so in cuprates we have the first ex-ample of 'electronic' BEC. This explains why Tc is so high. Near optimal doping, at the lowest temperatures almost all free carriers are paired and coherent within the superfluid. However, with increased doping, the fraction of uncondensed free fermions keeps growing, reaching 99% in heavily overdoped samples with $T_c = 5$ K, so any BEC description that involves only bosons also fails dramatically. It is in fact quite surprising that in an electron fluid a fraction of electrons are paired and shows behavior reminiscent of cold atom BEC.

The key experimental question is how much of this is universal for all known HTS compounds. To answer this, we need to repeat this type of study with other cuprates, electron- as well as hole-doped, including some with two and more CuO_2 planes in the structural unit. Then one should look beyond cuprates — at $(Ba,K)BiO_3$, pnictides, etc.

The ultimate motivation is the search for new HTS materials. From the present results, it appears that we should focus on increasing N_{s0} and decreasing m^*. Surprisingly, it appears beneficial to also increase T_0 (the vertical offset of the linear dependence in Fig. 3a). The grand challenge to the theory is to predict these quantities and lead the discovery of new superconductors.

ACKNOWLEDGEMENTS

REFERENCES

[1] Božović I., He X., Wu J. and Bollinger A. T., "The origin of high-temperature superconductivity in cuprates," Nature 536(7616), 309-311 (2016).
[2] He X., Gozar A., Sundling R. and Božović I., "High-precision measurement of magnetic penetration depth in superconducting films," Rev. Sci. Instr. 87, 113903 (2016).
[3] Lee, P. A., Nagaosa, N. and Wen, X. G., "Doping a Mott insulator: Physics of high-temperature superconductivity," Rev. Mod. Phys. 78, 17-85 (2006).
[4] Zaanen, J., Chakravarty, S., Senthil, T., Anderson, P. W., Lee, P., Schmalian, J., Imada, M., Pines, D., Randeria, M., Varma, C., Vojta, M. and Rice, M., "Towards a complete theory of high Tc," Nature Physics 2, 138-143 (2006).
[5] Keimer, B., Kivelson, S. A., Norman, M. R., Uchida, S. and Zaanen, J., "From quantum matter to high-temperature superconductivity in copper oxides," Nature 518, 179-186 (2015).

[6] Gao, L., Xue, Y. Y., Chen, F., Xiong, Q., Meng, R. L., Ramirez, D., Chu, C. W., Eggert, J. H. and Mao, H. K., "Superconductivity up to 164 K in $HgBa_2Ca_{m-1}Cu_mO_{2m+2+d}$ (m=1, 2, and 3) under quasi-hydrostatic pressures," Phys. Rev. B 50, 4260-4263 (1994).

[7] Damascelli, A., Hussain, Z. and Shen, Z.-X., "Angle-resolved photoemission studies of the cuprate superconductors," Rev. Mod. Phys. 75, 473–541 (2003).

[8] McElroy, K., Simmonds, R. W., Hoffman, J. E., Lee, D. H., Orenstein, J., Eisaki, H., Uchida, S. and Davis, J. C., "Relating atomic-scale electronic phenomena to wave-like quasi-particle states in superconducting $Bi_2Sr_2CaCu_2O_{8+\delta}$," Nature 422, 592-596 (2003).

[9] Proust, C., Boaknin, E., Hill, R. W., Taillefer, L. and Mackenzie, A. P., "Heat transport in a strongly overdoped cuprate: Fermi liquid and a pure d-wave BCS superconductor," Phys. Rev. Lett. 89, 147003 (2002).

[10] Laughlin, R. B., "Fermi-Liquid Computation of the Phase Diagram of High-Tc Cuprate Superconductors with an Orbital Antiferromagnetic Pseudogap," Phys. Rev. Lett. 112, 017004 (2014).

[11] Laughlin, R. B., "Hartree-Fock computation of the high-T_c cuprate phase diagram," Phys. Rev. B 89, 035134 (2014).

[12] Anderson, P. W., "The resonating valence bond state in La_2CuO_4 and superconductivity," Science 235, 1196–1198 (1987).

[13] Alen, P. B. and Mitrovic, B., "Theory of superconducting Tc", [Solid State Physics], Turnbull, D. and Ehrenreich, H., (editors), vol. 37, 1–92, Academic Press, New York (1982).

[14] Leggett, A. J., "Superfluidity," Rev. Mod. Phys. 71, S318-S323 (1999).

[15] Leggett, A. J., "The Ubiquity of Superconductivity," Annu. Rev. Condens. Matter. Phys. 2, 11-30 (2011).

[16] Bozovic, I., "Atomic-layer engineering of superconducting oxides: Yesterday, today, tomorrow," IEEE Trans. Appl. Supercond. 11, 2686–2695 (2001).

[17] Gozar A., Logvenov G., Fitting Kourkoutis L., Bollinger A. T., Giannuzzi L. A., Muller D. A., and Bozovic I., "Interface superconductivity between a metal and a Mott insulator," Nature 455, 782-785 (2008).

[18] Logvenov, G., Gozar, A. and Bozovic, I., "High-temperature superconductivity in a single copper-oxygen plane," Science 326, 699–702 (2009).

[19] Wu J., Pelleg O., Logvenov G., Bollinger A. T., Sun Y-J., Boebinger G. S., Vanević M., Radović Z. and Bozovic I., "Anomalous independence of interface superconductivity on carrier density," Nature Mater. 12, 877-881 (2013).

[20] Hebard, A. F. and Fiory, A. T., "Evidence for the Kosterlitz-Thouless transition in thin superconducting aluminum films," Phys. Rev. Lett. 44, 291–294 (1980).

[21] Claassen, J. H., Reeves, M. E. and Soulen, R. J. Jr., "A contactless method for measurement of the critical current density and critical temperature of superconducting rings," Rev. Sci. Instrum. 62, 996–1004 (1991).

[22] Clem, J. R. and Coffey, M. W., "Vortex dynamics in a type-II superconducting film and complex linear-response functions," Phys. Rev. B 46, 14662–14674 (1992).

[23] Turneaure, S. J., Ulm, E. R. and Lemberger, T. R., "Numerical modeling of a two-coil apparatus for measuring the magnetic penetration depth in superconducting films and arrays," J. Appl. Phys. 79, 4221-4227 (1996).

[24] Turneaure, S. J., Pesetski, A. A. and Lemberger, T. R., "Numerical modeling and experimental considerations for a two-coil apparatus to measure the complex conductivity of superconducting films," J. Appl. Phys. 83, 4334-4343 (1998).

[25] Gasparov, V. A. and Bozovic, I., "Magnetic field and temperature dependence of complex conductance of ultrathin $La_{1.65}Sr_{0.45}CuO_4/La_2CuO_4$ films," Phys. Rev. B 86, 094523 (2012).

[26] Kapitulnik, A., Palevski, A. and Deutscher, G., "Inhomogeneity effects on the magnetoresistance and the ghost critical field above T_c in thin mixture films of In-Ge," J. Phys. C: Solid State Phys. 18, 1305-1312 (1985).

[27] Breznay, N. P. and Kapitulnik, A., "Observation of the ghost critical field for superconducting fluctuations in a disordered TaN thin film," Phys. Rev. B 88, 104510 (2013).

[28] Shi X-Y., Logvenov G., Bollinger A. T., Božović I., Panagopoulos C. and Popović D., "Emergence of superconductivity from the dynamically heterogeneous insulating state in $La_{2-x}Sr_xCuO_4$," Nature Materials 12, 47-51 (2013).

[29] Pistolesi, F. and Strinati, G. C., "Evolution from BCS superconductivity to Bose condensation: Role of the parameter $k_F\xi$," Phys. Rev. B 49, 6356-6359 (1994).

[30] Pistolesi, F. and Strinati, G. C., "Evolution from BCS superconductivity to Bose condensation: Calculation of the zero-temperature phase coherence length," Phys. Rev. B 53, 15168-15192 (1996).

[31] Palestini, F. and Strinati, G. C., "Temperature dependence of the pair coherence and healing lengths for a fermionic superfluid throughout the BCS-BEC crossover," Phys. Rev. B 89, 224508 (2014).

[32] Uemura, Y. J. et al., "Universal Correlations between T_c and n_s/m^* (Carrier Density over Effective Mass) in High-Tc Cuprate Superconductors," Phys. Rev. Lett. 62, 2317-2320 (1989).

[33] Homes, C. C., et al., "A universal scaling relation in high-temperature superconductors," Nature 430, 539-541 (2004).

[34] Weinberg, S, "Superconductivity for Particular Theorists," Prog. Theor. Phys. Suppl. 86, 43-53 (1986).

[35] Leggett, A. J., "Diatomic molecules and Cooper pairs," [Modern Trends in the Theory of Condensed Matter], edited by Pekalski, A. and Przystawa, J. Lecture Notes In Physics 115, Springer Verlag, Berlin, 13-27 (1980).

[36] Chen, Q. J., Stajic, J., Tan, S. and Levin, K., "BCS-BEC crossover: From high temperature superconductors to ultracold superfluids," Physics Reports 412, 1-88 (2005).

[37] Chen, Q., Levin, K. and Stajic, J., "Applying BCS-BEC crossover theory to high-temperature superconductors and ultracold atomic Fermi gases," Low Temp. Phys. 32, 406-423 (2006).

[38] Randeria, M. and Taylor, E., "Crossover from Bardeen-Cooper-Schrieffer to Bose-Einstein Condensation and the Unitary Fermi Gas," Annu. Rev. Condens. Matter Phys. 5, 209-232 (2014).

[39] Cornell, E. A. and Wieman, C. E., "Bose-Einstein condensation in a dilute gas, the first 70 years and some recent experiments," Rev. Mod. Phys. 74, 875-893 (2002).

[40] Ketterle, W., "When atoms behave as waves: Bose-Einstein condensation and the atom laser," Rev. Mod. Phys. 74, 1131-1151 (2002).

[41] Greiner, M., Regal, C. A. and Jin, D. S., "Emergence of a molecular Bose-Einstein condensate from a Fermi gas," Nature 426, 537-540 (2003).

[42] Schunck, C. H., Shin, Y., Schirotzek, A. and Ketterle, W., "Determination of the fermion pair size in a resonantly interacting superfluid," Nature 454, 739-743 (2008).

[43] Ries, M. G., Wenz, A. N., Zürn, G., Bayha, L., Boettcher, I., Kedar, D., Murthy, P. A., Neidig, M., Lompe, T. and Jochim, S., "Observation of Pair Condensation in the Quasi-2D BEC-BCS Crossover," Phys. Rev. Lett. 114, 230401 (2015).

[44] Sommer, A. T., Cheuk, L. W., Ku, M. J. H., Bakr, W. S. and Zwierlein, M. W., "Evolution of Fermion Pairing from Three to Two Dimensions," Phys. Rev. Lett. 108, 045302 (2012).

[45] Fisher, D. S. and Hohenberg, P. C., "Dilute Bose gas in two dimensions," Phys. Rev. B 37, 4936-4943 (1988).

[46] Pilati, S., Giorgini, S. and Prokof'ev, N., "Critical temperature of interacting Bose gases in two and three dimensions," Phys. Rev. Lett. 100, 140405 (2008).

[47] Friedberg, R. and Lee, T. D., "Boson-Fermion model of superconductivity," Phys. Lett. A 138, 423-427 (1989).

[48] Alexandrov, A. S. and Mott, N. F., "Bipolarons," Rept. Prog. Phys. 57, 1197-128 (1994).

[49] Zhao, G. M., Hunt, M. B., Keller, H. and Muller, K. A., "Evidence for polaronic supercarriers in the copper oxide superconductors $La_{2-x}Sr_xCuO_4$," Nature 381, 676−678 (1996).

[50] Andreev, A. F., "Electron pairs for HTSC," JETP Letters 79, 88-90 (2004).

[51] Deutscher, G. and de Gennes, P.-G., "A spatial interpretation of emerging superconductivity in lightly doped cuprates," C. R. Physique 8, 937-41 (2007); Erratum, ibid. 9, 773 (2008).

[52] Micnas R., Ranninger J. and Robaszkiewicz S., "Superconductivity in narrow-band systems with local nonretarded attractive interactions," Rev. Mod. Phys. 62, 113-172 (1990).